

Cloning and Expression Study of the Mouse Tetrodotoxin-Resistant Voltage-Gated Sodium Channel α Subunit NaT/Scn11a

Katsuhisa Ogata,^{*,†} Seon-Yong Jeong,^{*,†} Hiroo Murakami,^{*,†} Hideji Hashida,^{*,†} Takashi Suzuki,^{†,‡} Naoki Masuda,^{*,†} Momoki Hirai,[§] Kyoko Isahara,[¶] Yasuo Uchiyama,[¶] Jun Goto,^{*,†,1} and Ichiro Kanazawa^{*,†}

^{*}Department of Neurology, Graduate School of Medicine, University of Tokyo, Tokyo 113-8655, Japan; [†]Core Research for Evolutional Science and Technology (CREST) Research Project, Japan Science and Technology Corporation, Saitama 332-0012, Japan; [‡]Department of Medical Zoology, Nagoya City Medical School, Aichi 467-8601, Japan; [§]Department of Integrated Biosciences, Graduate School of Frontier Sciences, University of Tokyo, Tokyo 113-0033, Japan; and [¶]Department of Cell Biology and Anatomy, Osaka University Medical School, Osaka 565-0871, Japan

Received November 8, 1999

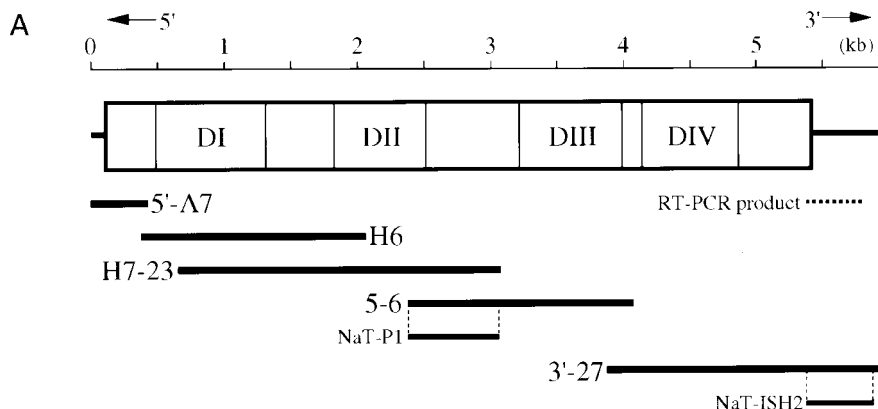
We have cloned a tetrodotoxin-resistant (TTX-R) voltage-gated sodium channel α subunit from a mouse cDNA library and designated it as NaT. It encodes 1765 amino acid residues and is virtually identical to that of Scn11a, which has been reported recently, except for 40 nt and 14 aa substitutions. The amino acid identity of NaT/Scn11a with rat NaN/SNS2 is 88%. NaT/Scn11a was mapped to mouse chromosome 9F3-F4 by fluorescence *in situ* hybridization (FISH). While rat NaN/SNS2 has been reported to be expressed specifically in the peripheral sensory neurons, NaT/Scn11a is expressed not only in the peripheral sensory neurons but also in the spinal cord, uterus, testis, ovary, placenta, and small intestine. NaT is detectable in mouse embryos 15 days postcoitus (p.c.), around the phase of organogenesis and gonadal differentiation. These findings demonstrate a unique distribution of NaT/Scn11a and suggest some of its roles in the above-mentioned processes. © 2000 Academic Press

The voltage-gated sodium channel is a membrane protein that plays a fundamental role in the rising phase of the action potential in most excitable cells such as neurons and muscle cells (1, 2). The channel is composed of one α subunit (~270 kDa) and one or two auxiliary subunits β 1 (~38 kDa) and β 2 (~33 kDa) (3). The α subunit mediates voltage-dependent gating and ion conductance, and the β subunits regulate the kinetic properties and facilitate membrane localization

of sodium channels (4, 5). There is a molecular diversity of α subunits (6, 7), and each α subunit is expressed in a tissue-specific and developmentally specific manner (8, 9).

Voltage-gated sodium channels are classified pharmacologically into two large groups according to their sensitivities to tetrodotoxin blocking (10). While most sodium channels are tetrodotoxin-sensitive (TTX-S), several clones have been reported to be resistant to tetrodotoxin (TTX-R). Those include rat Scn5a, human SCN5A (H1/SkM2/ μ 2), rat PN3/SNS, mouse Scn10a, human SCN10A, rat NaN/SNS2 and mouse Scn11a (6, 7). Scn5a and SCN5A are predominantly expressed in the heart (11). Rat PN3/SNS and NaN/SNS2 are expressed specifically in primary sensory neurons (12–15). Both TTX-S and TTX-R voltage-gated sodium currents have been observed in dorsal root ganglia (DRG) (16). PN3/SNS and NaN/SNS2 generate TTX-R currents in DRG neurons (15, 17). PN3/SNS shows a moderate level of amino acid identity of around 70% to the other α subunit molecules, while NaN/SNS2 exhibits less than 50% similarity to the other α subunit molecules, including PN3/SNS. Both PN3/SNS and NaN/SNS2 are expressed specifically in primary sensory neurons and are not detectable in the other neural and non-neural tissues in rats. While NaN/SNS2 is expressed in small-diameter neurons of DRG, PN3/SNS is expressed in small- and medium-diameter neurons. NaN/SNS2 is not detectable by day 15 of rat embryos, while PN3/SNS is expressed at that stage. Mouse Scn10a and human SCN10A are the orthologues of rat PN3/SNS (18, 19). Recently, mouse Scn11a has been reported to be the orthologue of rat NaN/SNS2 (20).

¹ To whom correspondence should be addressed. Fax: +81-3-5800-6548. E-mail: gotoj-tyk@umin.ac.jp.



B

MEERYYPVIFPPDERNFRPFT	FDSLAAIEKRITIQEKKKS	KDKAATEPQFRPQLDLKASR	60
KLPKLYGVDVPPDLIAKPLED	LDPFYKDHKTFMVLNKKRTI	YRFSAKRALFILGPFNPIRS	120
FMIRISVHSVFSMFIICTVI	INCMFMANNSSVDSRPSSNI	PEYVFIGIYVLEAVIKILAR	180
<div style="display: flex; justify-content: space-around;"> DI-S1 DI-S2 </div>			
GFIVDEFSYLRDPWNWLDLI	VIGTAIAPCFLGNKVNNLST	LRTFRVLRAKKAISVISGLK	240
<div style="display: flex; justify-content: space-around;"> DI-S3 DI-S4 </div>			
VIVGALLRSVKKLVDVMVLT	LFCLSFALVGQQLFMGILS	QKCIKDDCGNAPNSKDCFV	300
<div style="display: flex; justify-content: space-around;"> DI-S5 </div>			
KENDSEDFIMCGNLGRRSC	PDGSTCNKTTFNPDYNTNF	DSFGWSFLAMFRVMTQDSWE	360
<div style="display: flex; justify-content: space-around;"> DI-SS1 DI-SS2 </div>			
KLYRQILRTSGIYVFVFFVV	VIFLGSFYLLNLTLAVVTMG	YEEQNRNVAETEAKEKMFQ	420
<div style="display: flex; justify-content: space-around;"> DI-S6 </div>			
EAQQLLKEEKEALVAMGIDR	TSLNSLQASSFSPKKRKFFG	SKTRKSFFMRGSKTARASAS	480
DSEDDASKKPQLLEQTKRLS	QNLPELFDLHVDPLHRQRA	LSAVSILTITMQEQEKSQEP	540
CFPCGKNLASKYLVWECSP	WLCIKKVLQTIMTDPFTELA	ITICIIVNTVFLAMEHHNMD	600
<div style="display: flex; justify-content: space-around;"> DII-S1 </div>			
NSLKDILKIGNWVFTGIFIA	EMCLKIIALDPYHYFRHGWN	IPDSIVALVSLADVLFHKL	660
<div style="display: flex; justify-content: space-around;"> DII-S2 DII-S3 </div>			
KNLSFLASLRVLRVFKLAKS	WPTLNTLIKIIGHSVGALGN	LTVVLTIVVPIFSVVGMRLE	720
<div style="display: flex; justify-content: space-around;"> DII-S4 DII-S5 </div>			
GAKFNKTCSTSPESLRRRH	GDFYHSFLVVRILCGEWIE	TMWDCMQEMEGSPICVIVFV	780
<div style="display: flex; justify-content: space-around;"> DII-SS1 DII-SS2 </div>			
LIMVVGKLVVLNLFIALLLN	SFSNEEKDGNPEGETRKTIV	QLALDRFSRAFYFMARALQN	840
<div style="display: flex; justify-content: space-around;"> DII-S6 </div>			
FCRKRRCRRQNSPKPNEATES	FAGESRDTATLDTRSWKEYD	SEMTLYTGQAGAPLAPLAKE	900
EDDMCECCGECDAFPTSQPS	EAQACDLPLKTKRLPSFDDH	GVEMEVFSEEDFNLTIQSAR	960
KKSDAASMLSECSTIDLNDI	FRNLQKTVPQKQPDRCFPK	GLSCIFLCCCTIKKSPWVL	1020
WWIFRKTCYQIVKHSWFESF	IIFVILLSSGALILEDVNLP	SRPQVEKLLKCTDNIFTFIF	1080
<div style="display: flex; justify-content: space-around;"> DIII-S1 DIII-S2 </div>			
LLEMILKWVAFGRKYPTSA	WCWLDFLIIVVSVLSLTNLP	NLKSFRNLRALRPLRALSQF	1140
<div style="display: flex; justify-content: space-around;"> DIII-S3 DIII-S4 </div>			
EGMKVVVNALMSAIPAILNV	LLVCLIFWLFICILGVNFFS	GKFGRCINGTINKYFNASN	1200
<div style="display: flex; justify-content: space-around;"> DIII-S5 </div>			
VFNQSQCLVSNHTWKVPNVN	FDNVGNAYLALLQVATYKGW	LDIMNAAVDSRGKDEQPAFE	1260
<div style="display: flex; justify-content: space-around;"> DIII-SS1 DIII-SS2 </div>			
ANLYAYLYFVVFIIFGSFFT	LNLFIVGVIIDNPNQQQKLG	GQDIFMTEEQKKYNNAMKKL	1320
<div style="display: flex; justify-content: space-around;"> DIII-S6 </div>			
GTKKPQKPIPRPLNKCAQFV	FDLVTSQVFDVILGLIVTN	MIIMMAESEGPNEVQKIFD	1380
<div style="display: flex; justify-content: space-around;"> DIV-S1 </div>			
ILNIVFVVIPTVECLIKVFA	LRQHYFTNGWNLFDVVVVL	SIISTLVSGLENSNVFPPTL	1440
<div style="display: flex; justify-content: space-around;"> DIV-S2 DIV-S3 </div>			
FRIVRLARIGRIILRVRAAR	GIRTLFALMMSLPSLPNIG	LLLFLVMFIYAIFGMSWFSK	1500
<div style="display: flex; justify-content: space-around;"> DIV-S4 DIV-S5 </div>			
VKRGSGIDDIFNFDTFSGSM	LCLFQITTSAGWDALLNPML	ESKASCNSSSQESCQPPQIA	1560
<div style="display: flex; justify-content: space-around;"> DIV-SS1 DIV-SS2 </div>			
IYVFVSYYIISLLIVNMYI	AVILENFNTATEESEDPLGE	DDFEIFYEIEWKFDPEATQF	1620
<div style="display: flex; justify-content: space-around;"> DIV-S6 </div>			
IQYSSLSDFADALPEPLRVA	KPNRFQFLMMDLPMVMGDR	HCMVDVLAFTTRVLGNSSGL	1680
DTMKAMMEEFMEANPFKKL	YEPIVTTTKRKEEECAAVI	QRAYRRHMEKMIKLLKGRS	1740
SSSLQVFCNGDLSLDVFKI	KVHCD		1765

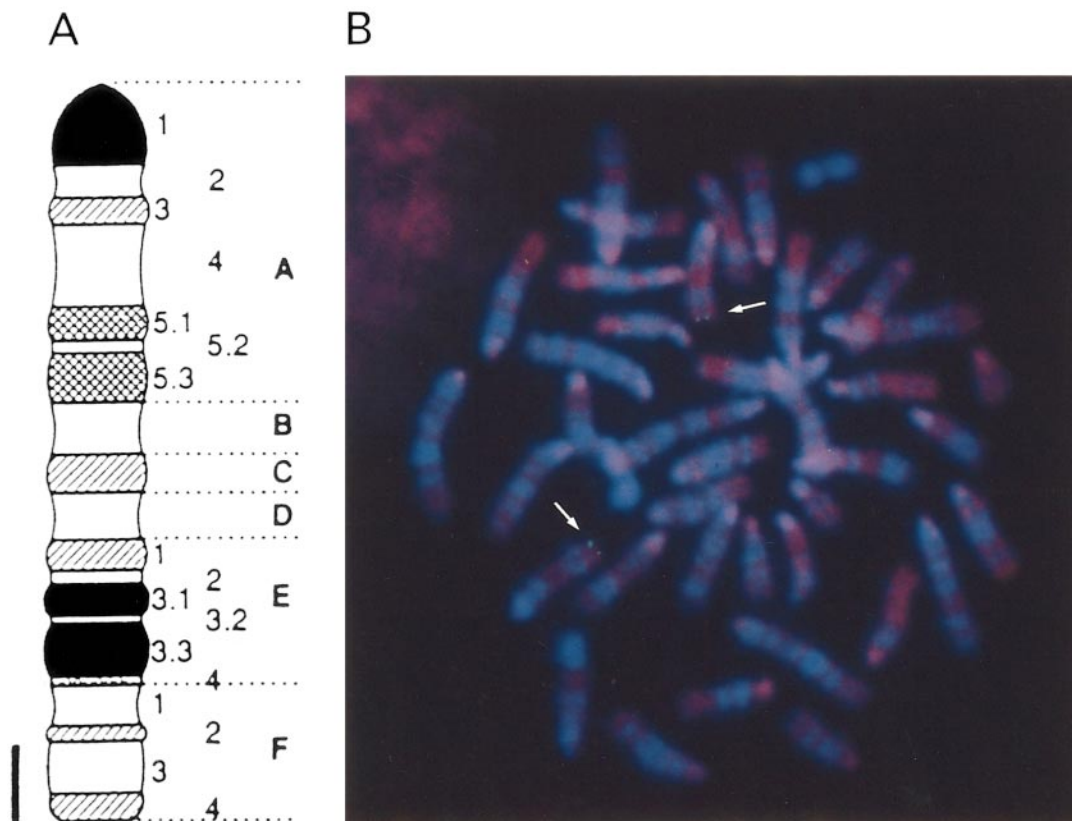


FIG. 2. Chromosomal mapping of NaT. (A) Idiogram of mouse chromosome 9. (B) Metaphase plate showing doublet signals on mouse chromosome 9F3-F4 (arrows). The biotinylated cDNA probe for NaT was hybridized to chromosomes with replication bands prepared from cultured splenocytes. After hybridization and washing, hybridization signals were amplified using rabbit anti-biotin (Enzo, NY) and fluorescein-labeled goat anti-rabbit IgG (Enzo, NY). The chromosomes were counterstained with propidium iodide. Double-exposure photomicrography was performed to visualize hybridization signals and G-banded chromosomes using a combination of WIBA and WU filter sets (Olympus).

We have independently cloned a mouse TTX-R voltage-gated sodium channel α subunit, designated as NaT, whose sequence is virtually identical to mouse NaN. Our studies revealed that NaT/Scn11a was expressed not only in DRG but also in spinal cord and non-neural tissues, in contrast to rat NaN, which was specific to DRG. In this report, we show cloning and mapping of NaT briefly and describe its expression in detail.

MATERIALS AND METHODS

RNA preparation and cDNA library construction. Total RNA was extracted using TRIZOL reagent (Gibco BRL), and mRNA was puri-

fied using an Oligotex-MAG mRNA purification kit (TaKaRa) from 500 mg of frozen eight-week-old normal BALB/c mouse testis tissue. First strand cDNA was synthesized using SuperScript II reverse transcriptase (Gibco BRL) with oligo(dT) and random primers. The cDNA library was constructed on a ZAP Express cDNA vector (Stratagene).

Nested PCR and RACE. Nested PCR was performed using an Expand High Fidelity PCR system (Roche Diagnostics), and the degenerate primers were as follows: Na5A, 5'-GTG GTS GGC ATG CAG CTS TTT GG-3'; Na5B, 5'-GAG TGG ATM GAG ACC ATG TGG GAC-3'; Na3A, 5'-TTC ATK GCR TTR TAG TAY TTC TTC TG; Na3B, 5'-GTT GAA RTT RTC WAT GAT GAC RCC AAT-3'. Na5A and Na3A were used for the first step PCR and Na5B and Na3B for the second PCR.

5' and 3' rapid amplification of cDNA ends (RACEs) were carried out using Marathon cDNA (Clontech) as a template. The NaT-

FIG. 1. Structure of mouse NaT/Scn11a. (A) Structure of the mouse NaT cDNA. The contig of the NaT clones are indicated. The dashed horizontal line indicates the position of the RT-PCR product. (B) Predicted amino acid sequences of mouse NaT. DI-DIV represents the four membrane-spanning domains, and the underlined S1-S6 and SS1-SS2 in individual domains indicate six putative α -helical transmembrane segments and the pore-lining segments, respectively. The serine residue in the SS2 of domain I, which is believed to underlie the TTX-R phenotype, is indicated in larger bold type (S358).

specific primers used for RACE were as follows: R5-A, 5'-GCT AGG ACG ACT GTC CAC AGA AG-3'; R5-B, 5'-TCT TGG CGC TGA AGC GAT AGA TTG TTC-3'; R3-A, 5'-CAA GTG GCG ACC TAT AAG GGC TGG CTG GAC-3'; R3-B, 5'-AAG ATG AGC AGC CGG CCT TTG AGG CGA ATC-3'. The PCR and RACE products were separated on 0.8% agarose gel. The DNA fragments of interest were subcloned into pBluescript II SK(+) (Stratagene).

Sequencing reactions were performed by the dideoxy nucleotide chain termination method, and an ABI PRISM 377 DNA Sequencer (Perkin Elmer) was used for analysis.

Fluorescence in situ hybridization (FISH). FISH was carried out using the methods described in previous reports (21, 22). The two subclones, 5-6 and H7-23, were used as probes (Fig. 1A).

Northern blot analysis. Mouse Multiple Choice Northern Blot (OriGene) and Mouse Embryo Multiple Tissue Northern Blot (Clontech) were purchased and used for Northern blot analysis. NaT-P1 (Fig. 1A) was used as a probe. After removal of NaT probes in 0.5% SDS, filters were rehybridized with labeled human β -actin cDNA as a control.

Reverse transcription (RT)-PCR. Two micrograms of total RNA of various tissues were extracted from eight-week-old ICR mice, as described above, and treated with RNase-free DNase I (Gibco BRL). Reverse transcription was performed using SupesScript II reverse transcriptase (Gibco BRL) with oligo(dT) primer. The PCR amplification was performed using Advantage cDNA polymerase mix (Clontech). The NaT-specific primers were 5'-GGA TGT GCC CAA GAT CAA GGT TCA TTG-3' and 5'-CAC CCA AAT CCG CAG CAC TGG TAG-3'. The mouse β -actin primers were as follows: 5'-CCA AGG CCA ACC GCG AGA AGA TGA C-3' and 5'-AGG GTA CAT GGT GGT GCC GCC AGA C-3'.

In situ hybridization. Sense and antisense digoxigenin (DIG)-labeled RNA probes were synthesized from NaT-P1 and NaT-ISH2 (Fig. 1A) using a DIG RNA Labeling Kit (Roche Diagnostics). The probes were hybridized with paraformaldehyde-fixed, dehydrated, paraffin-embedded and RNase-treated tissues according to the standard protocols. Tissues from eight-week-old ICR mice were hybridized with NaT-ISH2, and tissues from ten-week-old Wistar rats were hybridized with NaT-P1. Signals were detected using a DIG Nucleic Acid Detection Kit (Roche Diagnostics).

RESULTS AND DISCUSSION

Cloning, Sequence Analysis, and Chromosomal Mapping of NaT

To isolate mouse voltage-gated sodium channel α subunit clones, we initially performed nested PCR using the degenerate primers, Na5A, Na5B, Na3A and Na3B; those were designed based on highly conserved sequences among known sodium channel α subunits. The DNA fragments of 1.7 kb were subcloned and sequenced. Among the 20 clones examined, one clone was different from the others, which showed 87% nucleotide homology with rat NaN/SNS2 and 50~70% homology with other known sodium channels. We designated this clone as NaT (Fig. 1A). The other clones were identical to known sodium channels.

To obtain a full-length cDNA of NaT, approximately 10^6 pfu of the testis cDNA library were screened, and

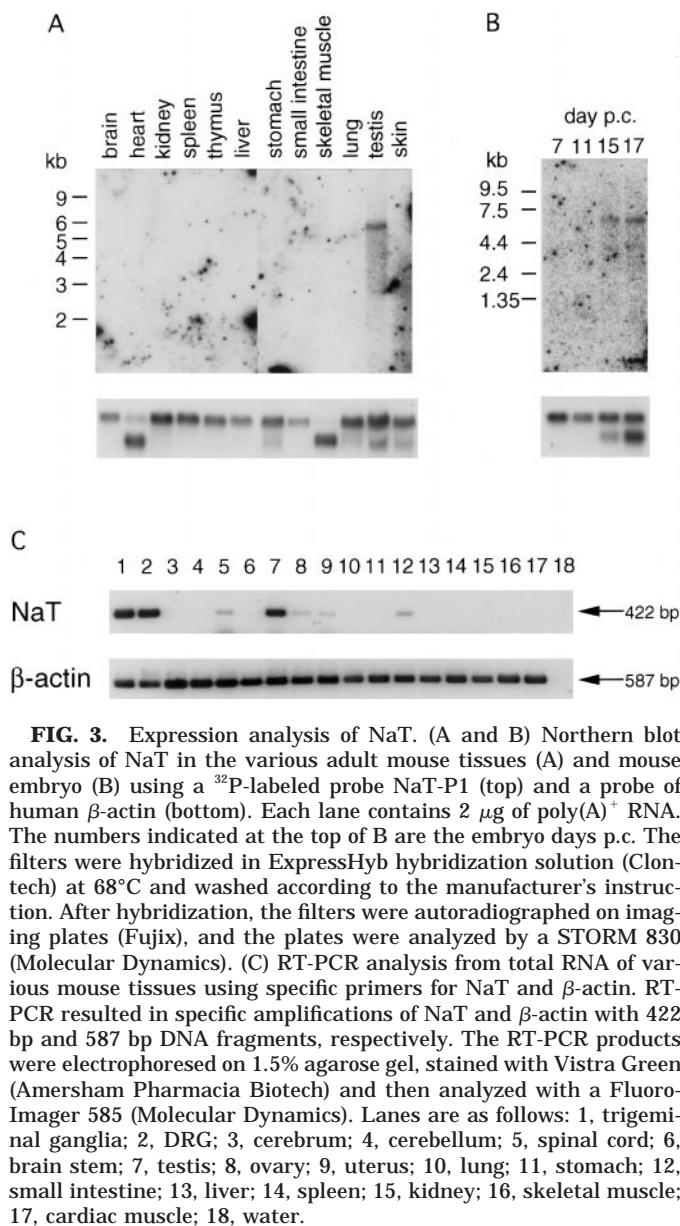


FIG. 3. Expression analysis of NaT. (A and B) Northern blot analysis of NaT in the various adult mouse tissues (A) and mouse embryo (B) using a 32 P-labeled probe NaT-P1 (top) and a probe of human β -actin (bottom). Each lane contains 2 μ g of poly(A)⁺ RNA. The numbers indicated at the top of B are the embryo days p.c. The filters were hybridized in ExpressHyb hybridization solution (Clontech) at 68°C and washed according to the manufacturer's instruction. After hybridization, the filters were autoradiographed on imaging plates (Fujix), and the plates were analyzed by a STORM 830 (Molecular Dynamics). (C) RT-PCR analysis from total RNA of various mouse tissues using specific primers for NaT and β -actin. RT-PCR resulted in specific amplifications of NaT and β -actin with 422 bp and 587 bp DNA fragments, respectively. The RT-PCR products were electrophoresed on 1.5% agarose gel, stained with VisTra Green (Amersham Pharmacia Biotech) and then analyzed with a Fluoro-Imager 585 (Molecular Dynamics). Lanes are as follows: 1, trigeminal ganglia; 2, DRG; 3, cerebrum; 4, cerebellum; 5, spinal cord; 6, brain stem; 7, testis; 8, ovary; 9, uterus; 10, lung; 11, stomach; 12, small intestine; 13, liver; 14, spleen; 15, kidney; 16, skeletal muscle; 17, cardiac muscle; 18, water.

two additional clones, H7-23 and H6, were obtained (Fig. 1A).

To determine the ends of NaT, 5' and 3' RACEs were carried out with the NaT-specific primers. Both 5' and 3' end clones were obtained; 5'-A7 for the 5'-end and 3'-27 for the 3'-end (Fig. 1A).

The longest open reading frame of NaT encodes 1,765 amino acid residues with a calculated molecular weight of 201 kDa (Fig. 1B, the DDBJ/EMBL/GenBank Accession Number is AB031389). The serine residue which determines the TTX-R phenotype is conserved in NaT (23, 24). The predicted amino acid sequence of NaT is aligned well with other mammalian sodium

channels, and it is identical to the mouse *Scn11a* that has been recently reported, except for 40 nucleotide and 14 amino acid substitutions (14, 20). These substitutions might arise from the difference of mouse strain employed. NaT and rat NaN/SNS2 show 89% nucleotide identity and 88% amino acid identity. NaT shows 40–60% similarity with the other known sodium channel α subunits.

FISH study revealed that specific hybridization signals for NaT were observed on chromosome 9F3-F4 (Fig. 2). This region is close to the loci of *Scn5a* and *Scn10a* and consistent with the previous report of the locus of mouse *Scn11a* (20). The mouse TTX-R sodium channel α subunit genes, *Scn5a*, *Scn10a*, and *Scn11a*, seem to be located on mouse chromosome 9 in a cluster.

Tissue-Specific and Developmentally Specific Expression of NaT

Each subtype of sodium channel is expressed in a tissue-specific and developmentally specific manner. We examined the distribution of NaT by Northern hybridization, RT-PCR and *in situ* hybridization.

Northern blot hybridization revealed that the size of NaT mRNA was approximately 6.0 kb, which was compatible with the size of the cDNA. The gene was predominantly expressed in the testes, and no signal was detectable in any of the other mouse tissues examined (Fig. 3A).

RT-PCR was carried out with the NaT-specific primers of the C-terminal and 3'UTR (dashed line in Fig. 1A). That experiment demonstrated that NaT was expressed not only in the testis but also in the trigeminal ganglia, DRG, spinal cord, ovary, uterus and small intestine (Fig. 3C).

To examine the expression of NaT in detail, *in situ* hybridization was carried out with mouse and rat tissues. To avoid cross-hybridization with other sodium channels, NaT-P1 and NaT-ISH2, which were specific for NaT, were used (Fig. 1A). Mouse tissues were hybridized with NaT-ISH2 containing 3'UTR that has a lower similarity to the other sodium channel α subunits than the coding region. Rat tissues were hybridized with NaT-P1. This probe contains the intracellular loop L2 region that shows the lowest similarity to the other sodium channel α subunits, it is but highly conserved in the orthologous genes among different species (16). *In situ* hybridization showed that NaT was expressed in the DRG, spinal cord, uterus, testis, ovary, placenta and small intestine (Fig. 4). No hybridization signal was detected with the sense probe in any of the tissues

examined. A similar distribution of expression was observed in rats (data not shown).

NaT is expressed in small-diameter neurons in mouse DRG, and this is the same as in rat NaN/SNS2 (14, 15). Since small-diameter neurons in DRG include nociceptive cells, NaT/*Scn11a* might be concerned with the pain pathway (16). In addition, our study demonstrated the expression of NaT/*Scn11a* in spinal neurons. The signals were relatively strong in ventral large-diameter neurons that were presumably motor neurons. Although it has been reported that the TTX-R sodium channel *Scn5a* is expressed in spinal cord astrocytes, no expression of TTX-R sodium channel has been demonstrated in neurons of the spinal cord.

The expression of NaT was hardly detectable in skeletal or cardiac muscles. RT-PCR showed the expression of NaT in the small intestine and uterus, which included smooth muscles. *In situ* hybridization revealed that NaT was not expressed in the muscle layer of the small intestine.

In the small intestine, NaT was expressed in goblet cells. Goblet cells are intestinal epithelial cells that are short-lived and constantly renewed; they secrete mucus. In epithelial cells, a nonvoltage-gated sodium channel is expressed, but no voltage-gated sodium channel expression has been reported.

NaT was expressed in both male and female gonads and placenta. Hybridization signals were detected in spermatogonia and spermatocytes in the testes, in granular cells surrounding oocytes and in syncytiotrophoblasts in the placenta. Expression and function of the sodium channel in gonads remains obscure.

We examined the developmental profile of NaT expression by Northern hybridization of mouse embryos. NaT was detectable in mouse embryos 15 days postcoitus (p.c.) (Fig. 3B). After gastrulation, organogenesis takes place in the mouse embryo beginning 9 days p.c. (25). DRG arise from neural crest cells that are derived from the neural plate and migrate away from the neural tube after neural tube closure (26). In mouse embryos, neural tube closure is completed around 9.5 days p.c., and DRG differentiate beginning 10 days p.c. Germ cells enter the gonadal ridges at 10–11 days p.c., and the differences in the gonadal ridges of male and female embryos can be detected initially around 12.5 days p.c. NaT becomes detectable during the organogenesis when DRG arise and gonads differentiate into the appropriate sex.

We reported here a TTX-R sodium channel α subunit, NaT/*Scn11a*, the expression of which is uniquely distributed in the neurons, gonads and epithelial cells in the small intestine.

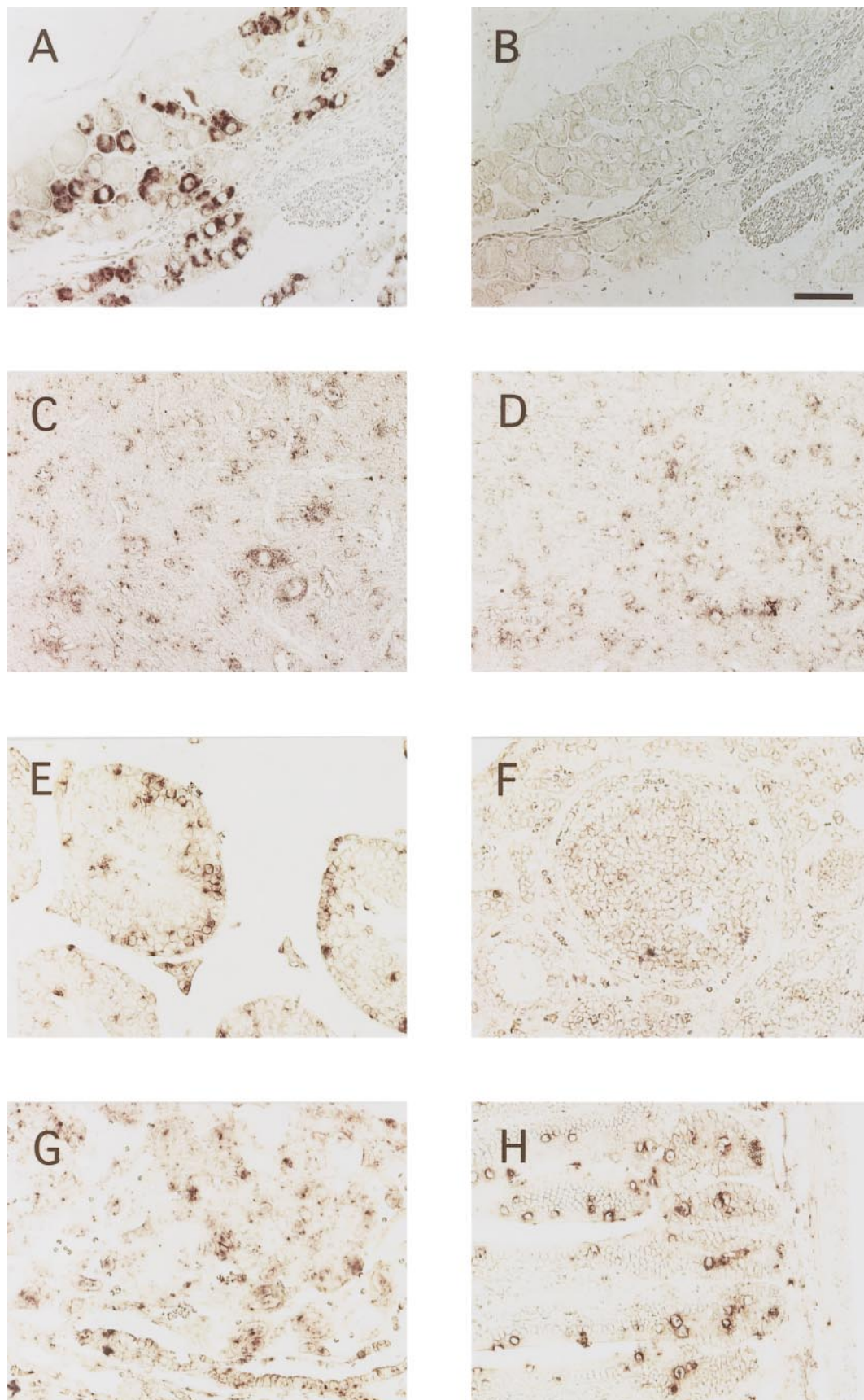


FIG. 4. *In situ* hybridization analysis of NaT in mouse tissues. Sections show the DRG (A), spinal cord (C, ventral; D, dorsal), testis (E), ovary (F), placenta (G), and small intestine (H) with antisense riboprobe. No hybridization signal was present with sense riboprobe in any of the tissues examined (e.g., in DRG; B). The bar indicates 50 μ m.

ACKNOWLEDGMENTS

This work was supported by a grant from the CREST, Japan Science and Technology Corporation, and a grant from the Ministry of Health and Welfare of Japan.

REFERENCES

1. Catterall, W. A. (1992) *Physiol. Rev.* **72**, S15–S48.
2. Noda, M. (1993) *Ann. N. Y. Acad. Sci.* **707**, 20–37.
3. Isom, L. L., De Jongh, K. S., and Catterall, W. A. (1994) *Neuron* **12**, 1193–1194.
4. Goldin, A. L., Snutch, T., Lubbert, H., Dowsett, A., Marshall, J., Auld, V., Downey, W., Fritz, L. C., Lester, H. A., Dunn, R., Catterall, W. A., and Davidson, N. (1986) *Proc. Natl. Acad. Sci. USA* **89**, 554–558.
5. Isom, L. L., Scheuer, T., Brownstein, A. B., Ragsdale, D. S., Murphy, B. J., and Catterall, W. A. (1995) *J. Biol. Chem.* **270**, 3306–3312.
6. Plummer, N. W., and Meisler, M. H. (1999) *Genomics* **57**, 323–331.
7. Goldin, A. L. (1999) *Ann. N. Y. Acad. Sci.* **868**, 38–50.
8. Beckh, S., Noda, M., Lubbert, H., and Numa, S. (1989) *EMBO J.* **8**, 3611–3616.
9. Mandel, G. (1992) *J. Membr. Biol.* **125**, 193–205.
10. Catterall, W. A. (1980) *Annu. Rev. Pharmacol. Toxicol.* **20**, 15–43.
11. Gellens, M., George, A., Chen, L., Chahine, M., Horn, R., Barchi, R., and Kallen, R. (1992) *Proc. Natl. Acad. Sci. USA* **89**, 554–558.
12. Akopian, A. N., Sivilotti, L., and Wood, J. N. (1996) *Nature* **379**, 257–262.
13. Sangameswaran, L., Delgado, S. G., Fish, L. M., Koch, B. D., Jakeman, L. B., Stewart, G. R., Sze, P., Hunter, J. C., Eglen, R. M., and Herman, R. C. (1996) *J. Biol. Chem.* **271**, 5953–5956.
14. Dib-Hajj, S. D., Tyrrell, L., Black, J. A., and Waxman, S. G. (1998) *Proc. Natl. Acad. Sci. USA* **95**, 8963–8968.
15. Tate, S., Benn, S., Hick, C., Trezise, D., John, V., Mannion, R. J., Costigan, M., Plumptre, C., Grose, D., Gladwell, Z., Kendall, G., Dale, K., Bountra, C., and Woolf, C. J. (1998) *Nat. Neurosci.* **1**, 653–655.
16. Waxman, S. G., Cummins, T. R., Dib-Hajj, S., Fjell, J., and Black, J. A. (1999) *Muscle Nerve* **22**, 1177–1197.
17. Akopian, A. N., Souslova, V., England, S., Okuse, K., Ogata, N., Ure, J., Smith, A., Kerr, B. J., McMahon, S. B., Boyce, S., Hill, R., Stanfa, L. C., Dickenson, A. H., and Wood, J. N. (1999) *Nat. Neurosci.* **2**, 541–548.
18. Souslova, V. A., Fox, M., Wood, J. N., and Akopian, A. N. (1997) *Genomics* **41**, 201–209.
19. Rabert, D. K., Koch, B. D., Illick, M., Oberholte, R. A., Naylor, S. L., Herman, R. C., Eglen, R. M., Hunter, J. C., and Sangameswaran, L. (1998) *Pain* **78**, 107–114.
20. Dib-Hajj, S. D., Tyrrell, L., Escayg, A., Wood, P. M., Meisler, M. H., and Waxman, S. G. (1999) *Genomics* **59**, 309–318.
21. Matsuda, Y., Harada, Y., Natsuume-Sakai, S., Lee, K., Shiomi, T., and Chapman, V. M. (1992) *Cytogenet. Cell Genet.* **61**, 282–285.
22. Hirai, M., Suto, Y., and Kanoh, M. (1994) *Cytogenet. Cell Genet.* **66**, 149–151.
23. Satin, J., Kyle, J. W., Chen, M., Bell, P., Cribbs, L. L., Fozzard, H. A., and Rogart, R. B. (1992) *Science* **256**, 1202–1205.
24. Sivilotti, L., Okuse, K., Akopian, A. N., Moss, S., and Wood, J. N. (1997) *J. Neurosci.* **15**, 3231–3242.
25. Hogan, B., Costantini, F., and Lacy, E. (1986) *in* Manipulating the Mouse Embryo, a Laboratory Manual, pp. 19–70, Cold Spring Harbor Laboratory, New York.
26. Wolpert, L., Beddington, R., Brockes, J., Jessell, T., Lawrence, P., and Meyerowitz, E. (1998) Principles of Development, Oxford Univ. Press, Oxford, UK.